

Edge-Reconstructed, Few-Layered Graphene Nanoribbons: Stability and Electronic Properties

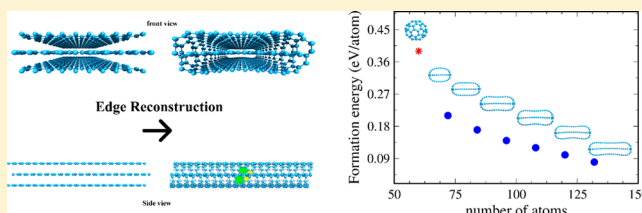
Juliana A. Gonçalves,[†] Regiane Nascimento,[†] Matheus J. S. Matos,[†] Alan B. de Oliveira,[†] Hélio Chacham,[‡] and Ronaldo J. C. Batista^{*,†}

[†]Departamento de Física, Universidade Federal de Ouro Preto, Campus Morro do Cruzeiro, 35400-000, Ouro Preto, MG Brazil

[‡]Departamento de Física, ICEX, Universidade Federal de Minas Gerais, CP 702, 30123-970, Belo Horizonte, MG Brazil

S Supporting Information

ABSTRACT: We report a first-principles study of edge-reconstructed, few-layered graphene nanoribbons. We find that the nanoribbon stability increases linearly with increasing width and decreases linearly with increasing number of layers (from three to six layers). Specifically, we find that a three-layer 1.3 nm wide ribbon is energetically more stable than the C₆₀ fullerene, and that a 1.8 nm wide ribbon is more stable than a (10,0) carbon nanotube. The morphologies of the reconstructed edges are characterized by the presence of five-, six-, and sevenfold rings, with sp³ and sp² bonds at the reconstructed edges. The electronic structure of the few-layered nanoribbons with reconstructed edges can be metallic or semiconducting, with band gaps oscillating between 0 and 0.28 eV as a function of ribbon width.



1. INTRODUCTION

In the last years carbon materials have attracted the attention of many researchers. Materials such as graphene,¹ fullerenes,² carbon nanotubes,³ and hybrids of these allotropes^{4,5} have shown a large potential for applications in several fields, such as medicine, engineering, and nanotechnology.^{6–16} All this intensive study devoted to carbon allotropes is due to their outstanding properties, which include high mechanical strength (both for graphene and nanotubes), the unique electronic structure, and high carrier mobility, which can reduce the switching time of graphene-based transistors.^{14,15}

Nanotube ends and graphene edges are respectively the 1D and 2D analogues of surfaces in 3D solids. Nonreconstructed graphene edges should present dangling-bond like states associated with undercoordinated carbon atoms. Because dangling-bond terminated borders are usually unstable, reconstructions and adsorption of chemical species from the environment are not rare to occur. Many studies, both experimental^{17–22} and theoretical,^{18,23–26} have been carried out in the field of edges reconstruction in graphene and graphite. Koskinen et al.²³ have investigated planar reconstruction patterns in both zigzag and armchair graphene edges. Their results show that zigzag graphene edges are metastable and reconstruction spontaneously happens at room temperature, provided that amount of hydrogen surrounding the sample is low. Edge reconstruction in graphite was also studied by Rotkin and Gogotsi.²⁴ Their transmission electron microscopy (TEM) images show few-layer edges surrounded by nanoarch structures.

In this work we propose a new type of edge reconstruction for nonpassivated graphene nanoribbons with the number of layers varying from three up to six. We employed first-

principles calculations to investigate structural and electronic properties of such structures. This work is organized as follows. Methodology and computational details are given in Section 2. Results regarding energetic stability and electronic structure are given in Section 3. Section 4 ends the text with our conclusions.

2. CALCULATION DETAILS

We performed calculations based on the density functional theory (DFT) as implemented in both SIESTA²⁷ and Quantum-ESPRESSO²⁸ code. For the SIESTA calculations we have used the generalized gradient approximation (GGA), proposed by Perdew, Burke, and Ernzerhof (PBE).²⁹ As exchange-correlation functional, and also the fully nonlocal functional, which takes into account the van der Waals interactions, as proposed by Klimes, Bowler, and Michaelides (VDW-KBM).³⁰ We make use of norm-conserving Troullier–Martins³¹ pseudopotentials in the Kleinman–Bylander³² factorized form. Also, we have used as basis set the standard double- ζ plus polarizations orbitals (DZP). The basis functions and the electron density were projected into a uniform real space grid defined by the energy cutoff of 200 Ry. We set a $3 \times 3 \times 85$ Monkhorst–Pack³³ grid for integrations over the Brillouin zone. All structures were optimized up to where the forces on each atom were smaller than 0.02 eV/Å. For the Quantum-ESPRESSO calculations we used ultrasoft pseudopotentials: the Perdew–Burke–Ernzerhof (PBE)²⁹ formulation of the GGA approximation. The kinetic energy cutoff was 30 Ry for the electronic wave functions and 300 Ry for the

Received: January 17, 2017

Revised: February 22, 2017

Published: February 27, 2017

electron density. The structures were relaxed with the tolerance for forces of 0.02 eV/Å on each atom. Fermi–Dirac smearing was used to define the electronic occupations at room temperature in constructing the electron density from Kohn–Sham orbitals. The employed unit cells, Figure 1, are periodic

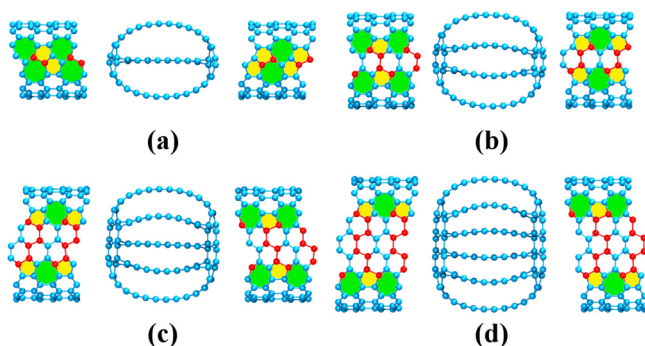


Figure 1. Geometries of graphene armchair nanoribbons with reconstructed edges. The panels show the front and side views of the nanoribbons with reconstructed edges (two units cells are shown in each panel for clarity). Panels (a), (b), (c), and (d) show respectively the nanoribbons with 3, 4, 5, and 6 layers. All structures present the same number of pentagonal and heptagonal rings, which connect the outmost layers to the nanoribbon inner layers. The number of sp^3 increases linearly with the number of layers. The red spheres represent sp^3 hybridized carbon atoms. The inner carbon atoms were removed in the side view image for reasons of clarity.

over the nanoribbons length with lattice constant six times the C–C bond length. In the other directions we have used vectors large enough to avoid the interaction between the periodic images. In the next section we present our DFT results and specify which methodology was used in each calculation.

3. RESULTS AND DISCUSSION

3.1. Energetic Stability. Reconstructed edges in graphite were first reported by Rotkin and Gogotsi.²⁴ Their TEM images show few-layer edges surrounded by nanoarch structures. The original analysis of Rotkins and Gogotsi focused on the surrounding nanoarches. Here we will focus on possible edge reconstructions of the few-layer edges that do not form arches. Specifically, we will consider few-layer armchair nanoribbons that contain the reconstructions on both edges. The geometries of the reconstructed nanoribbons are shown in Figure 1. These reconstructions appeared spontaneously in simulations of the rupture of a few-layer graphene/nanotube composite system under tensile strain, as shown in the Supporting Information file. The geometries of the reconstructed nanoribbons are shown in Figure 1. The geometries of the studied nanoribbons are shown in Figure 1, where it can be seen that all structures present lines of pentagonal (yellow region) and heptagonal (green region) rings along the nanoribbon length. Those lines connect the two outmost layers of the nanoribbons to its inner layers. Such a connection is provided by two atoms of the pentagonal ring that make four covalent C–C bonds. Thus, unlike the case of the Stone–Wales defect,^{26,34} the atoms of the pentagonal and heptagonal rings do not lie in the same plane. In the three-layered nanoribbons, Figure 1a, pentagons and heptagons of the upper and lower layers share a common side. In all other cases—panels b–d—the pentagonal rings of the upper and lower layers are connected by zigzag lines of sp^3 hybridized carbon

atoms (red spheres). Parallel to them, zigzag lines of sp^2 hybridized carbon atoms connect heptagons of the upper layer to heptagons of the lower layer. Those lines form a surface similar to that of the diamond (110) surface, where the half of the atoms that are sp^2 hybridized lie in a different plane from that of sp^3 hybridized atoms, and reflect the fact that the ribbons have armchair edges prior to reconstruction.

In order to investigate the energetic stability of the structures, we calculated the formation energy according to eq 1

$$\frac{E_f}{n_C} = \frac{1}{n_C}(E_{\text{total}} - n_C\mu_C) \quad (1)$$

where E_{total} and n_C are the total energy and the number of C atoms for each studied system, respectively. μ_C is the chemical potential for C atoms, which was defined as the total energy per atom of perfect graphene sheet.

Figure 2 shows, as red dots, the formation energy per atom as a function of the number of carbon atoms in structures a–d of

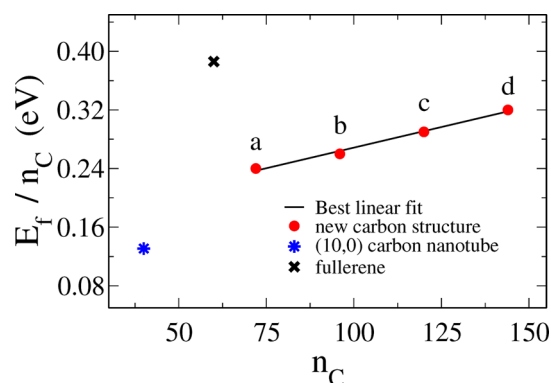


Figure 2. Red dots: formation energies per atom as a function of the number of atoms in the unit cell of the few-layer graphene nanoribbons with the same width ($W \approx 1.14$ nm) and reconstructed edges shown in Figure 1. The dots are calculated data, and the line is the best linear fit with angular and linear constants 0.0011 eV/atom² and 0.156 eV/atom, respectively. For the sake of comparison, we also show the formation energy per atom of the C_{60} and the (10,0) carbon nanotube.

Figure 1. The figure shows that the formation energy per atom of the proposed structures increases with the number of atoms or layers in the structures. Such a behavior can be understood if one considers $E_f \propto n_{sp^3}$, where n_{sp^3} is the number of sp^3 bonds in the structure. The ratio n_{sp^3}/n_C increases with increasing n_C , and for a small number of layers it is roughly linear, which leads to the roughly linear behavior shown in Figure 2. In addition, the distance between successive layers at the nanoribbon edge ($d_{\text{edge}} \leq 3$ Å) is smaller than graphite interlayer distance ($d_{\text{graphite}} \approx 3.3$ Å). Thus, the edges compress the graphene layers between them, which also contributes to the increase in formation energy with increasing N (number of layers). Such increase must be also linear with N ($\Delta E \propto N(d_{\text{graphite}} - d_{\text{edge}})$). Interestingly, Figure 2 also shows that all nanoribbons present formation energies per atom between those of the C_{60} fullerene (0.39 eV/atom) and the (10,0) carbon nanotube (0.13 eV/atom), which suggests that those new reconstructed edges can be observed experimentally.

The structures shown in Figure 1 correspond to very thin nanoribbons, of width $W = 1.14$ nm. In order to investigate the dependence of the properties of the ribbons as a function of width, we systematically increased the width of the three-

layered nanoribbons, as shown in Figure 3, and computed their formation energy per atom according to eq 1. The values of

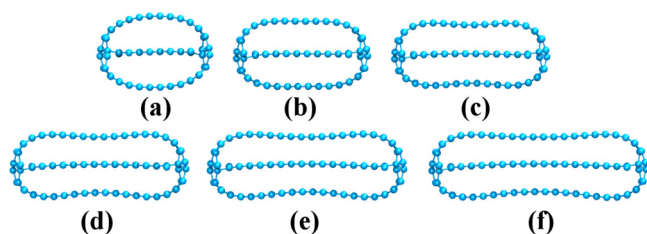


Figure 3. Geometries of three-layered graphene nanoribbons with different widths. The width and number of atoms in the structures shown in the panels (a)–(f) are respectively $W \approx 1.14$ nm, 72; $W \approx 1.39$ nm, 84; $W \approx 1.64$ nm, 96; $W \approx 1.89$ nm, 108; $W \approx 2.14$ nm, 120; and $W \approx 2.38$ nm, 132.

formation energy, calculated with different DFT implementations, are shown in Table 1. It can be seen that the structure with 120 atoms, Figure 3e, is as energetically stable as the (10,0) carbon nanotube (see Table 1 for PBE-LCAO).

Table 1. Formation Energy per Number of C Atoms of the Structures Shown in Figure 3 Calculated Using Different DFT Implementations^a

n_C	E_f (eV/atom)		
	PBE-LCAO	VDW-LCAO	PBE-PW
40 (nanotube)	0.13	0.13	0.16
60 (fullerene)	0.39	0.39	0.41
72	0.23	0.21	0.29
84	0.19	0.17	0.26
96	0.16	0.14	0.23
108	0.14	0.12	
120	0.13	0.10	
132	0.11	0.08	

^aPBE-LCAO stands for calculations using the PBE semilocal functional and a localized basis set as implemented in SIESTA. VDW-LCAO stands for calculations using the nonlocal functional of Klimes, Bowler, and Michaelides and the SIESTA localized basis set. PBE-PW stands for calculations using the PBE functional and a nonlocal plane wave basis set as implemented in Quantum-Expresso.

If the description of the weak dispersive forces is improved by the use of a nonlocal functional (VDW-LCAO), values for the nanoribbons formation energy systematically decrease in comparison to those predicted by PBE calculations. The VDW-LCAO calculations predict that the three-layered structure with 108 atoms is energetically more stable than the (10,0) nanotube. We have also performed DFT calculations with a plane-wave basis set (PBE-PW) for selected structures. We obtain values of formation energy consistent with those calculated using a localized basis set.

The values shown in Table 1 are plotted as a function of inverse of the number of atoms in Figure 4, where a linear behavior can be observed. Such a behavior can be understood if we assume that the formation energy of those structures can be written as

$$E_f = 2A + Bn_C \quad (2)$$

where A is the energy cost associated with one of the two reconstructed edges (which does not depend on the nanoribbon width) and B is the energy per carbon atom of the three-

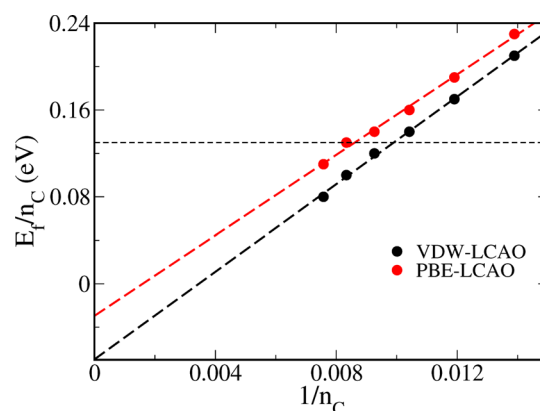


Figure 4. Formation energy per atom as a function of the inverse of number of atoms of the three-layered graphene nanoribbons shown in Figure 3. From the linear fitting we obtain $A = 9.27$ eV and $B = -0.03$ eV/atom for PBE-LCAO and $A = 10.08$ eV and $B = -0.07$ eV/atom for VDW-LCAO. The horizontal line indicates the formation energy of a (10,0) nanotube.

layer graphene. Such an expression fits very well the calculated data, as can be seen in Figure 4. This figure shows that the reconstructed edges have a constant energy cost no matter the size of the ribbon.

3.2. Electronic Structure. We have investigated the electronic structure of the structures shown in Figure 3 using the ab initio approach implemented in the SIESTA, where the VDW-KBM was used as the exchange-correlation potential. The obtained results (see Figure 5) show that the nanoribbons

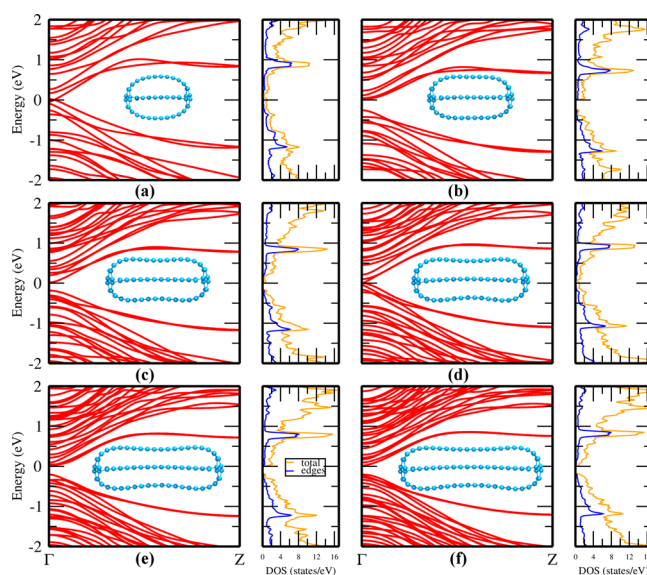


Figure 5. Band structure along with the density of states (DOS) of the three-layered graphene nanoribbons depicted in Figure 3. The orange line corresponds to total DOS of the systems, and the blue one represents the DOS projected at the C atoms that form the heptagonal and pentagonal rings at the edges.

with reconstructed edges can be either metallic or semiconductor, depending on their width. Such results suggest that sp^3 bonds might act like nodal points of the standing wave in the zigzag direction, making the electronic structure of each layer similar to that of single graphene nanoribbons. The picture of sp^3 bonds behaving like nodal points of the wave

vectors along the ribbon width is consistent with the predictions of Nakada et al.³⁵ for the band gaps of armchair nanoribbons. In particular, the $P = 3M - 1$ rule for metallicity of armchair nanoribbons mentioned in the Nakada work is satisfied by the reconstructed armchair nanoribbons proposed in this work. Within this rule, the armchair ribbon is metallic whenever M is an integer number (P is the number of dimer lines in a armchair ribbon). The upper and lower layers of narrowest reconstructed nanoribbon investigated in this work contain $P = 14$ dimer lines (Including the sp^3 bonds), and as can be seen in Figure 5, such ribbon is metallic. The reconstructed nanoribbons shown in panels b, c, d, e, and f of Figure 5 contain 16, 18, 20, 22, and 24 dimer lines, respectively. It can be seen that among those ribbons only the one with $P = 20$ is metallic, in agreement with the rule prediction. In a more specific way, the band gap of graphene armchair nanoribbons can be also divided into three groups^{36,37} depending on their width (for nanoribbons which can be seen as unfolded single wall nanotubes $W = (n + 1/2)0.246$ nm, where n is an integer). Those groups are the $n = 3i$, the $n = 3i + 1$, and the $n = 3i + 2$ groups, where i is an integer. Note that the first group presents the smallest band gap values (in some cases band gap is even absent), the second one shows intermediate values, and the third the largest ones. This leads to a band gap as a function of the nanoribbon's width with oscillating behavior with a period of $3n$. A behavior similar to that of graphene nanoribbon is observed in Figure 6, where the band gaps of the structures

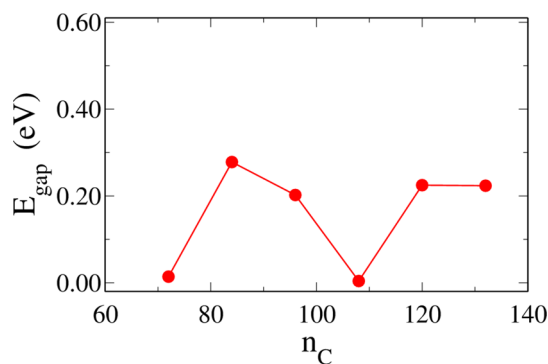


Figure 6. Band gaps as a function of the number of atoms of the three-layered structures depicted in Figure 3. Lines connecting symbols are meant to guide the eyes.

shown in Figure 3 are shown as a function of the number of atoms (which is proportional to nanoribbons width). Such a result is consistent with the presence of nodal points at the edges. Another result that indicates that sp^3 bonds act like nodal points is the absence of electron states at the edge atoms near the Fermi level for all structures (Figure 5).

4. CONCLUSION

We employed different implementations of first-principles methods to investigate the structural and electronic properties of few-layered graphene nanoribbons with reconstructed edges. We propose a type of reconstruction where pairs of pentagonal and heptagonal rings connect graphene layers through sp^2 and sp^3 bonds. We found that narrow nanoribbons with reconstructed edges are energetically more stable than the C_{60} fullerene, in spite of the presence of sp^3 bonds. Due to the interaction between layers, the proposed structures become more stable with increasing width. As a result, a 1.89 nm wide,

three-layered nanoribbon with reconstructed edges is energetically more stable than a (10,0) carbon nanotubes. Our results suggest that the sp^3 bonds at the edges act as nodal points of wave functions along the nanoribbon width, which results in an oscillatory behavior of the band gap as a function of nanoribbon width, with either metallic or semiconductor behavior.

■ ASSOCIATED CONTENT

Supporting Information

The Supporting Information is available free of charge on the ACS Publications website at DOI: 10.1021/acs.jpcc.7b00532.

Calculations which provide the structures investigated in this work (ZIP)

Description of the system (graphene/carbon nanotube) (PDF)

■ AUTHOR INFORMATION

Corresponding Author

*E-mail: batista.rjc@gmail.com. Phone: +55 (31) 3559 1667.

Notes

The authors declare no competing financial interest.

■ ACKNOWLEDGMENTS

We acknowledge the support from the Brazilian Science agencies CNPq, FAPEMIG, CAPES, and the project INCT de Nanomateriais de Carbono. A.B.O., M.J.S.M., and R.J.C.B. thank PROPP-UFOP for the Auxílio Financeiro a Pesquisador-Custeio 2016 grant. R.N. thanks CAPES for her postdoc fellowship.

■ REFERENCES

- (1) Novoselov, K. S.; Geim, A. K.; Morozov, S. V.; Jiang, D.; Zhang, Y.; Dubonos, S. V.; Grigorieva, I. V.; Firsov, A. A. Electric Field Effect in Atomically Thin Carbon Films. *Science* **2004**, *306*, 666–669.
- (2) Kroto, H. W.; Heath, J. R.; O'Brien, S. C.; Curl, R. F.; Smalley, R. E. C_{60} : Buckminsterfullerene. *Nature* **1985**, *318*, 162–163.
- (3) Iijima, S. Helical Microtubules of Graphitic Carbon. *Nature* **1991**, *354*, 56–58.
- (4) Kim, N. D.; Li, Y.; Wang, G.; Fan, X.; Jiang, J.; Li, L.; Ji, Y.; Ruan, G.; Hauge, R. H.; Tour, J. M. Growth and Transfer of Seamless 3D Graphene–Nanotube Hybrids. *Nano Lett.* **2016**, *16*, 1287–1292.
- (5) Batista, R. J.; Carara, S. S.; Manhobosco, T. M.; Chacham, H. A Ferromagnetic Pure Carbon Structure Composed of Graphene and Nanotubes: First-Principles Calculations. *J. Phys. Chem. C* **2014**, *118*, 8143–8147.
- (6) Fan, Z.; Yan, J.; Zhi, L.; Zhang, Q.; Wei, T.; Feng, J.; Zhang, M.; Qian, W.; Wei, F. A Three-Dimensional Carbon Nanotube/Graphene Sandwich and Its Application as Electrode in Supercapacitors. *Adv. Mater.* **2010**, *22*, 3723–3728.
- (7) Wang, Y.; Li, Y.; Tang, L.; Lu, J.; Li, J. Application of Graphene-Modified Electrode for Selective Detection of Dopamine. *Electrochem. Commun.* **2009**, *11*, 889–892.
- (8) Bakry, R.; Vallant, R. M.; Najam-ul Haq, M.; Rainer, M.; Szabo, Z.; Huck, C. W.; Bonn, G. K. Medicinal Applications of Fullerenes. *Int. J. Nanomed.* **2007**, *2*, 639–649.
- (9) Avouris, P. Graphene: Electronic and Photonic Properties and Devices. *Nano Lett.* **2010**, *10*, 4285–4294.
- (10) Yang, K.; Feng, L.; Shi, X.; Liu, Z. Nano-Graphene in Biomedicine: Theranostic Applications. *Chem. Soc. Rev.* **2013**, *42*, 530–547.
- (11) Yang, W.; Thordarson, P.; Gooding, J. J.; Ringer, S. P.; Braet, F. Carbon Nanotubes for Biological and Biomedical Applications. *Nanotechnology* **2007**, *18*, 412001.
- (12) De Heer, W. A.; Chátelain, A.; Ugarte, D. A Carbon Nanotube Field-Emission Electron Source. *Science* **1995**, *270*, 1179–1180.

- (13) Harrison, B. S.; Atala, A. Carbon Nanotube Applications for Tissue Engineering. *Biomaterials* **2007**, *28*, 344–353.
- (14) Schwierz, F. Graphene Transistors. *Nat. Nanotechnol.* **2010**, *5*, 487–496.
- (15) Bolotin, K. I.; Sikes, K.; Jiang, Z.; Klima, M.; Fudenberg, G.; Hone, J.; Kim, P.; Stormer, H. Ultrahigh Electron Mobility in Suspended Graphene. *Solid State Commun.* **2008**, *146*, 351–355.
- (16) Chen, Z.; Mao, R.; Liu, Y. Fullerenes for Cancer Diagnosis and Therapy: Preparation, Biological, and Clinical Perspectives. *Curr. Drug Metab.* **2012**, *13*, 1035–1045.
- (17) Kim, K.; Coh, S.; Kisielowski, C.; Crommie, M.; Louie, S. G.; Cohen, M. L.; Zettl, A. Atomically Perfect Torn Graphene Edges and Their Reversible Reconstruction. *Nat. Commun.* **2013**, *4*, 2723.
- (18) Koskinen, P.; Malola, S.; Häkkinen, H. Evidence for Graphene Edges beyond Zigzag and Armchair. *Phys. Rev. B: Condens. Matter Mater. Phys.* **2009**, *80*, 073401.
- (19) Liu, Z.; Suenaga, K.; Harris, P. J.; Iijima, S. Open and Closed Edges of Graphene Layers. *Phys. Rev. Lett.* **2009**, *102*, 015501.
- (20) Huang, J. Y.; Ding, F.; Yakobson, B. I.; Lu, P.; Qi, L.; Li, J. In Situ Observation of Graphene Sublimation and Multi-Layer Edge Reconstructions. *Proc. Natl. Acad. Sci. U. S. A.* **2009**, *106*, 10103–10108.
- (21) Jia, X.; Hofmann, M.; Meunier, V.; Sumpter, B. G.; Campos-Delgado, J.; Romo-Herrera, J. M.; Son, H.; Hsieh, Y.-P.; Reina, A.; Kong, J.; et al. Controlled Formation of Sharp Zigzag and Armchair Edges in Graphitic Nanoribbons. *Science* **2009**, *323*, 1701–1705.
- (22) Jia, X.; Campos-Delgado, J.; Gracia-Espino, E. E.; Hofmann, M.; Muramatsu, H.; Kim, Y. A.; Hayashi, T.; Endo, M.; Kong, J.; Terrones, M.; et al. Loop Formation in Graphitic Nanoribbon Edges Using Furnace Heating or Joule Heating. *J. Vac. Sci. Technol. B* **2009**, *27*, 1996–2002.
- (23) Koskinen, P.; Malola, S.; Häkkinen, H. Self-Passivating Edge Reconstructions of Graphene. *Phys. Rev. Lett.* **2008**, *101*, 115502.
- (24) Rotkin, S.; Gogotsi, Y. Analysis of Non-Planar Graphitic Structures: from Arched Edge Planes of Graphite Crystals to Nanotubes. *Mater. Res. Innovations* **2002**, *5*, 191–200.
- (25) Huang, B.; Liu, M.; Su, N.; Wu, J.; Duan, W.; Gu, B.-l.; Liu, F. Quantum Manifestations of Graphene Edge Stress and Edge Instability: A First-Principles Study. *Phys. Rev. Lett.* **2009**, *102*, 166404.
- (26) Lee, G.-D.; Wang, C.; Yoon, E.; Hwang, N.-M.; Ho, K. Reconstruction and Evaporation at Graphene Nanoribbon Edges. *Phys. Rev. B: Condens. Matter Mater. Phys.* **2010**, *81*, 195419.
- (27) Soler, J. M.; Artacho, E.; Gale, J. D.; Garcia, A.; Junquera, J.; Ordejón, P.; Sánchez-Portal, D. The SIESTA Method for ab Initio Order-N Materials Simulation. *J. Phys.: Condens. Matter* **2002**, *14*, 2745.
- (28) Giannozzi, P.; Baroni, S.; Bonini, N.; Calandra, M.; Car, R.; Cavazzoni, C.; Ceresoli, D.; Chiarotti, G. L.; Cococcioni, M.; Dabo, I.; et al. QUANTUM ESPRESSO: A Modular and Open-Source Software Project for Quantum Simulations of Materials. *J. Phys.: Condens. Matter* **2009**, *21*, 395502.
- (29) Perdew, J. P.; Burke, K.; Ernzerhof, M. Generalized Gradient Approximation Made Simple. *Phys. Rev. Lett.* **1996**, *77*, 3865–3868.
- (30) Klimeš, J.; Bowler, D. R.; Michaelides, A. Chemical Accuracy for the van der Waals Density Functional. *J. Phys.: Condens. Matter* **2010**, *22*, 022201.
- (31) Troullier, N.; Martins, J. L. Efficient Pseudopotentials for Plane-Wave Calculations. *Phys. Rev. B: Condens. Matter Mater. Phys.* **1991**, *43*, 1993–2006.
- (32) Kleinman, L.; Bylander, D. M. Efficacious Form for Model Pseudopotentials. *Phys. Rev. Lett.* **1982**, *48*, 1425–1428.
- (33) Monkhorst, H. J.; Pack, J. D. Special Points for Brillouin-Zone Integrations. *Phys. Rev. B* **1976**, *13*, 5188–5192.
- (34) Stone, A. J.; Wales, D. J. Theoretical Studies of Icosahedral C₆₀ and Some Related Species. *Chem. Phys. Lett.* **1986**, *128*, 501–503.
- (35) Nakada, K.; Fujita, M.; Dresselhaus, G.; Dresselhaus, M. S. Edge State in Graphene Ribbons: Nanometer Size Effect and Edge Shape Dependence. *Phys. Rev. B: Condens. Matter Mater. Phys.* **1996**, *54*, 17954–17961.
- (36) Wassmann, T.; Seitsonen, A. P.; Saitta, A. M.; Lazzeri, M.; Mauri, F. Clar's Theory, π -Electron Distribution, and Geometry of Graphene Nanoribbons. *J. Am. Chem. Soc.* **2010**, *132*, 3440–3451.
- (37) Yan, Q.; Huang, B.; Yu, J.; Zheng, F.; Zang, J.; Wu, J.; Gu, B.-L.; Liu, F.; Duan, W. Intrinsic Current–Voltage Characteristics of Graphene Nanoribbon Transistors and Effect of Edge Doping. *Nano Lett.* **2007**, *7*, 1469–1473.